Journal of Thermal Analysis and Calorimetry, Vol. 74 (2003) 789–799

SYNTHESIS, CHARACTERIZATION AND THERMAL DECOMPOSITION STUDIES OF SOME MALATES COORDINATION COMPOUNDS

Part I. Iron-nickel compounds

O. Carp [1*], *L. Patron* [1], *I. Mindru* [1], *G. Marinescu* [1], *L. Diamandescu* [2] *and A. Banuta* [2]

[1]Institute of Physical Chemistry, Splaiul Independentei nr. 202, Sector 6, Bucharest, Romania
[2]Institute of Atomic Physics, National Institute of Materials Physics, P. O. Box MG-7, Bucharest, Romania

(Received April 8, 2002; in revised form July 10, 2003)

Abstract

The thermal behaviour of three coordination compounds, potential precursors of nickel ferrite $[Fe_2Ni(C_4H_4O_5)_{2.5}(OH)_2]NO_3{\cdot}5H_2O$,$[Fe_2Ni(C_4H_8O_3N_2)_4](NO_3)_8{\cdot}24H_2O$ and $(NH_4)[Fe_2Ni(C_4H_4O_5)_3(OH)_3]{\cdot}3H_2O$ has been investigated to evaluate their suitability as precursors for nickel ferrite. For a complete and reliable assignment of the thermal transformations, the isolable solid intermediates and end products were characterized by IR, X-ray diffraction and Mössbauer investigations. A decomposition scheme is proposed.

Keywords: iron-nickel coordination compound, nickel ferrite, thermal analysis

Introduction

The synthesis of mixed oxides through thermal decomposition of polynuclear coordination compounds represents a versatile and predictable method, due to the possibility of controlling the quality (compositional and microstructural) of the end products features, by selecting suitable ligands and outer coordination sphere ions [1–3]. Several studies have been performed using different ligands selected from the carboxylate acids class [4–7]. Their use in mixed oxides precursors has become a subject of interest because of their complexing ability and ease of removal non-toxic gases. The use of the malic ion, $^{-}OOC–CH_2(OH)–CH_2–COO^{-}$ is a relatively uninvestigated route [8–14].

The aim of the present study is to determine the thermal behaviour of some iron-nickel malates coordination compounds, in order to determine how small changes in their nature may influence the course of thermal decompositions and quality of the final mixed oxide.

---

[*] Author for correspondence: E-mail: carp@apia.ro

1388–6150/2003/ $ 20.00

Akadémiai Kiadó, Budapest
Kluwer Academic Publishers, Dordrecht

Experimental

Compounds preparation

As starting materials, $Fe(NO_3)_3 \cdot 9H_2O$, $Ni(NO_3)_2 \cdot 6H_2O$ and malic acid of reagent grade, in $2Fe^{3+}$:$1Ni^{2+}$:4 malic acid ratio were used. As variable synthesis parameters the pH and reaction medium were chosen. While in aqueous medium at pH~2–3 and ~4.5–5$[Fe_2Ni(C_4H_4O_5)_{2.5}(OH)_2]NO_3 \cdot 5H_2O$ (**I**) and $[Fe_2Ni(C_4H_8O_3N_2)_4](NO_3)_8 \cdot 24H_2O$ (**II**) compounds were formed, an ethanol reaction medium and a pH of ~4.5–5 favor the isolation of $(NH_4)[Fe_2Ni(C_4H_4O_5)_3(OH)_3] \cdot 3H_2O$ (**III**) compound. The compounds were characterized by elemental chemical analysis: the metal and (C, H, N) content was determined by atomic absorption and microcombustion techniques. $Fe_2NiC_{10}H_{22}N_1O_{22.5}$ Anal. calcd/found: Fe%: 15.98/16.32; Ni%: 8.42/8.56; C%: 16.83/16.58; H%: 2.14/2.55; N%: 2.81/2.31. $Fe_2NiC_{16}H_{80}N_{16}O_{60}$ Anal. calcd/found: Fe%: 6.88/6.84; Ni%: 3.63/3.60; C%: 11.80/11.91; H%: 4.92/4.93; N%: 13.76/13.75. $Fe_2NiC_{12}H_{25}N_1O_{21}$ Anal. calcd/found: Fe%: 16.23/16.23; Ni%: 8.55/8.35; C%: 20.86/28.65; H%: 3.62/3.52; N%: 2.02/2.01.

Diffuse reflectance spectra (400–1000 nm) were recorded at room temperature on a Specord M-40 spectrophotometer using MgO as standard. IR spectra (400–4000 cm^{-1}) were recorded with a BIO-RAD FTIR 125 type spectrophotometer, in KBr pellets. The X-ray powder investigations were performed DRON–3 diffractometer, with CoK_α radiation. Mössbauer spectra were obtained at room temperature with a constant acceleration spectrometer (PROMEDA type equipment) using a 10 mCi Co^{57} (Rh) source. The thermal measurements (TG, DTG, DTG) were performed using a Q-1500 D Paulik–Paulik–Erdey derivatograph in a static air atmosphere.

Results and discussion

Characterization of the coordination compounds

The corresponding IR spectra of the three compounds (Table 1) suggest that malic acid is coordinated to the metal ions through both its two COO^- and C–OH groups. This statement is supported by the split of the free acid carboxylic group band (~1730 cm^{-1}) into two very strong bands characteristic for coordinated carboxylic group, ($\nu_{OCOasym}$ ~1600 cm^{-1} and ν_{OCOsym} ~1380–1390 cm^{-1}), and by the shift towards lower frequencies (1120 $cm^{-1} \rightarrow$1040–1100 cm^{-1}) of the band assigned to $\nu_{(C\text{-}OH)}$. The band appearing in the range of 600–500 cm^{-1}, can be attributed to M–O stretching vibration.

For compound (**I**), the splitting of $\nu_{OCOasym}$ and ν_{OCOsym} vibrations lead to values of the magnitude of separation $\Delta\nu=\nu_{asym}-\nu_{sym}$, equal with $\Delta\nu_1$=240 cm^{-1} and respectively 150 cm^{-1}. Such results suggest two different coordination mode of COO^- group. On the basis of spectroscopic criteria [15], the magnitude of separation $\Delta\nu=\nu_{asym}-\nu_{sym}$ may represent an indication for establishing the different coordination mode of the carboxylate ions. So, $\Delta\nu$ values included in the range 140–160 cm^{-1}, higher than those observed for ionic compounds ($\Delta Na_2(C_4H_4O_5)$=180 cm^{-1}) suggest a bridging bidentate bonding. On the other hand, values of $\Delta\nu$>180 cm^{-1} are characteristic for unidentate coordination compounds. For the same compound the IR spectrum evidenced four peaks between 600–440 cm^{-1}, outcome which indicate the pres-

Table 1 Representative IR frequencies (cm^{-1}) of the three coordination compounds and their decomposition products

Assignment	$[Fe_2Ni(C_4H_4O_5)_{2.5}(OH)_2]NO_3\cdot 5H_2O$					
	cc*	200°C	270°C	300°C	400°C	500°C
ν(OH) hydroxyl			3650 w 3627 w	3644 w 3626 w		
ν(OH) water	3427 br	3430 br	3430 br	3429 w	3430 w	3400 vw
$\nu(NH_4)^+$ammonium						
$\nu(NH_2)$						
$\nu(CO_2)$			2360 w	2360 s	2360 s	2360 w
ν_{asym}(COO) carboxylate	1652 s	1638 m	1649 vw			
$\nu(CO_3)$ carbonate				1390 m	1394 m	
ν_{sym}(COO) carboxylate	1390 s	1381 m	1397 w			
$\sigma(CH_3)$ acetate			1380 sh			
$\nu(NO_3)$ nitrate	1309 m					
$\rho(CH_3)$ acetate			1070 w	1068 vw		
σ(OH)	1041 w	1042 vw	1020 w	1020 w		
$\nu(CO_3)$ carbonate				870 m	870 w	
$\nu(NO_3)$ nitrate	804 w 700 w					
$\nu(CO_3)$ carbonate				670 m	668 w	
ν(M–O)	593 w 536 w 479 w 440 w	600 w 500 w	600 w 500 w	590 vs	595 vs 418 m	595 vs 420 m
	$(NH_4)[Fe_2Ni(C_4H_4O_5)_3(OH)_3]\cdot 3H_2O$					
	cc*	150°C	200°C	250°C	300°C	400°C
ν(OH) hydroxyl			3653 w 3680 w	3658 vw	3658 vw	
ν(OH) water	3422 br	3420 br	3420 br	3420 br	3420 br	3429 vw
$\nu(NH_4)^+$ ammonium	~3300 br					
$\nu(NH_2)$						
$\nu(CO_2)$			2362 vs	2360 vs	2360 vs	2360 s
ν_{asym}(COO) carboxylate	1622 s	1630 s	1630 m			
$\nu(CO_3)$ carbonate			1542 vw			
ν_{sym}(COO) carboxylate	1401 m	1401 m	1387 vw			
$\sigma(CH_3)$ acetate		~1378 sh				
$\nu(NO_3)$ nitrate						

Table 1 Continued

	$(NH_4)[Fe_2Ni(C_4H_4O_5)_3(OH)_3]\cdot 3H_2O$					
	cc*	150°C	200°C	250°C	300°C	400°C
ρ(CH_3) acetate			1080 w			
σ(OH)	1041 w		1041 w	1050 vw	1051 vw	
ν(CO_3) carbonate				669 w		
ν(NO_3)nitrate						
ν(CO_3)carbonate						
ν(M–O)	536 w	600 w	600 w	600 w 418 w	600 w 418 w	600 vs 418 w

Assignment	$[Fe_2Ni(C_4H_8N_2O_3)_4(NO_3)_8]\cdot 24H_2O$				
	cc*	170°C	210°C	300°C	400°C
ν(OH) hydroxyl		3658 w	3658 vw	3658 w	
ν(OH) water	3421 br	3420 br	3420 w br	3420 w br	3429 vw
$\nu(NH_4)^+$ammonium					
ν(NH_2)	3158 n				
ν(CO_2)		2360 vs	2360 vs	2360 vs	2360 s
ν_{asym}(COO) carboxylate	1607 s	1650 m	1611 vw		
ν(CO_3) carbonate		1444 sh	1542 vw	1547 vw	
ν_{sym}(COO) carboxylate	1382 s	1388 m	1387 vw		
σ(CH_3) acetate		1360 sh		1381 w	
ν(NO_3) nitrate	1287 sh				
ρ(CH_3) acetate		1100 w			
σ(OH)	1042 w		1050 vw	1051 vw	
ν(CO_3) carbonate					
ν(NO_3) nitrate	832 w 694 w				
ν(CO_3) carbonate		668 m	669 m	668 m	680 vw
ν(M–O)	598 w 530 w	583 w 418 w	600 w 418 w	600 w 418 w	600 vs 418 w

*Coordination compound
br – broad, vs – very strong, s – strong, m – medium, w – weak, vw – very weak

ence of dissimilar bonds M–O. This finding associated to the fractional coefficient of the malic anion suggests that this compound may exist in a polymeric form.

The electronic spectra evidenced that both metallic ions exhibit an octahedral environment [16]. The bands identified at 660–750 nm and ~460 nm are characteristic for

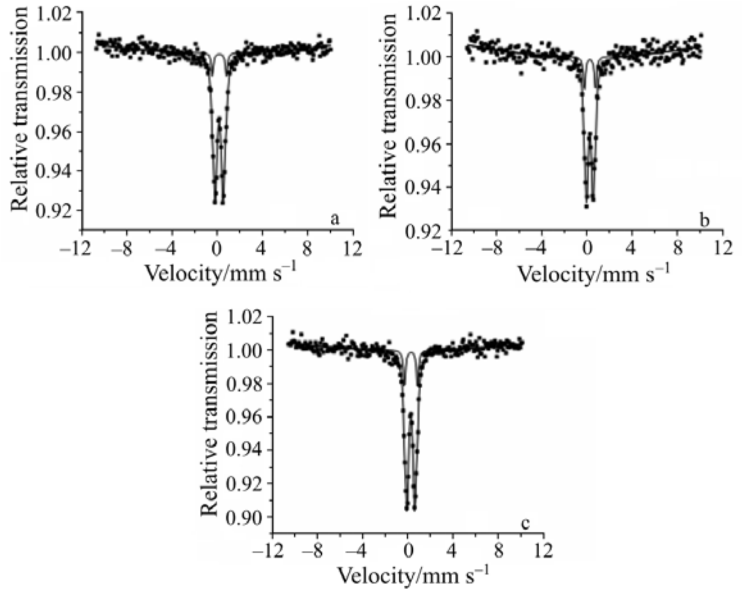

Fig. 1 Mössbauer spectra of the polynuclear compounds
a – $[Fe_2Ni(C_4H_4O_5)_{2.5}(OH)_2]NO_3{\cdot}5H_2O$; b – $[Fe_2Ni(C_4H_8O_3N_2)_4](NO_3)_8{\cdot}24H_2O$
and c – $(NH_4)[Fe_2Ni(C_4H_4O_5)_3(OH)_3]{\cdot}3H_2O$

Ni(II) (d^8), being assigned to the ν_2 ($^3T_{1g}(F){\leftarrow}^3A_{2g}$) and ν_3 ($^3T_{1g}(P){\leftarrow}^3A_{2g}$) transitions in an O_h, high spin environment. For Fe(III)(d^5) in a high-spin octahedral environment, the forbidden spin transition bands $^4A_{1g}$,$^4E_g(G){\leftarrow}^6A_{1g}$ and $^4T_{1g}(G){\leftarrow}^6A_{1g}$ are identified at 370 and 540 nm.

Table 2 Mössbauer hyperfine parameters of the investigated coordination compounds

Sample	IS*/ mm s^{-1}	QS**/ mm s^{-1}	Relative areas/ %	Site assignment
$[Fe_2Ni(C_4H_4O_5)_{2.5}(OH)_2]NO_3{\cdot}$ $5H_2O$ (**I**)	0.27	0.71	91.5	Fe^{3+}, high spin, octa
	0.30	1.25	8.5	Fe^{3+}, high spin, distorted octa
$[Fe_2Ni(C_4H_8O_3N_2)_4(NO_3)_8]{\cdot}$ $24H_2O$ (**II**)	0.28	0.56	85.8	Fe^{3+}, high spin, octa
	0.29	1.00	14.2	Fe^{3+}, high spin, distorted octa
$(NH_4)[Fe_2Ni(C_4H_4O_5)(OH)_3]{\cdot}$ $3H_2O$ (**III**)	0.27	0.69	86.3	Fe^{3+}, high spin, octa
	0.29	1.16	13.3	Fe^{3+}, high spin, distorted octa
Errors	±0.01	±0.02	±0.7	

*isomer shift, **quadrupolar splitting QS

The presence of Fe^{3+} in two distinct octahedral environments is revealed by the Mössbauer spectra (Fig. 1 and Table 2). A higher nonequivalence is evidenced for compound (**I**) (higher ΔQS value).

Non-isothermal analysis of the compounds

Thermal behaviour of $[Fe_2Ni(C_4H_4O_5)_{2.5}(OH)_2]NO_3\cdot5H_2O$

The thermal curves (Fig. 2a) reveal four decomposition steps. The first endothermic dehydration (75–150°C) corresponding to 5 water molecules evolving (calcd/found 13.15/12.87%) accompanied by the decrease of the specific absorption bands is followed by a step (150–240°C) assigned to the degradation of nitrate anions and malate oxidative fragmentation with a malonate intermediate formation (calcd./found 18.71/16.70%). The presence of malonates as intermediates of malates decomposition was reported by earlier studies [10,17]. The IR spectra (Table 1) evidenced the disappearance of the bands assigned to NO_3^- and HO^- groups.

The next decomposition step of a mass loss of 33.91% (240–320°C) represents the malonate lattice breakdown. The decomposition progresses through an acetate intermediate (bands characteristic to CH_3 group at 1100–1000 cm^{-1} and shoulder at ~1380 cm^{-1}) leading to a mixture containing beside the main product nickel ferrite (Fe_2NiO_4) small amounts of iron and nickel compounds. So, Ni, $NiCO_3$ (IR bands at 1400 and 668 cm^{-1}), FeOOH as lepidocrit (crystallographic less developed, IR bands at 3650 and 3627 and 1100 cm^{-1} characteristic for OH group) and γ-Fe_2O_3 (crystallographically poorly definable phase) are discerned. Two observations are important to be made. Firstly, an acetate intermediate is iden-

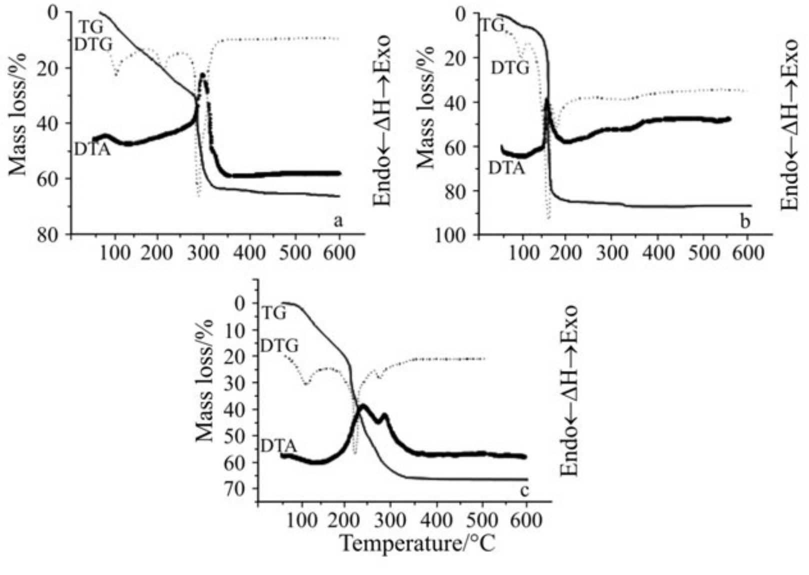

Fig. 2 Thermoanalytical curves (TG, DTG and DTA) of the polynuclear compounds a – $[Fe_2Ni(C_4H_4O_5)_{2.5}(OH)_2]NO_3\cdot5H_2O$, b – $[Fe_2Ni(C_4H_8O_3N_2)_4](NO_3)_8\cdot24H_2O$ and c – $(NH_4)[Fe_2Ni(C_4H_4O_5)(OH)_3]\cdot3H_2O$ (heating rate of 5°C min^{-1})

tified also in the decomposition of monometallic malonates coordination compounds [12,18]. Secondly, the presence of $NiCO_3$ may be explained as following: carbonaceous moieties are oxidized on the NiO surface, with concomitant reduction of the oxide to the metal. Since the process is conducted in air in the presence of CO_2 formerly evolved, the metal undergoes rapid reoxidation and carbonation. At 2630 cm^{-1} a band assigned to the asymmetric mode of CO_2 is evidenced, suggesting its presence in a trapped state into the solid matrix. At higher temperatures (335–595°C) a gradual mass loss (1.13%), assigned to $NiCO_3$ decomposition. The X-ray patterns of the intermediates obtained at 400°C indicate the presence of traces belonging to FeOOH, γ-Fe_2O_3, Ni and $NiCO_3$ beside Fe_2NiO_4. The Mössbauer spectrum of this decomposition product, consist mainly in a superposition of three magnetic sextets corresponding to different iron sites in the lattice (Fig. 3a). The two extreme sextets are characteristics for nickel ferrite [19, 20] (with a relative abundance of about 44%) and correspond respectively to the iron ions in tetrahedral sites (A) and respectively octahedral sites (B). The third sextet exhibits a collapsed magnetic hyperfine structure probably due superparamagnetic effects that are characteristic for small magnetic particles. X-ray diffraction data infer the presence of FeOOH and γ-Fe_2O_3 phases in this decomposition product, which in small particles could be responsible for the collapsed sextet in Mössbauer spectrum of sample.

In the temperature range 300–500°C the reaction progress is accompanied by the shifts of spinel most intensive line 311 (Fig. 4): firstly to lower 2θ values (300–400°C), secondly to higher ones (400–500°C). This behaviour suggest that in the initial spinelic structure, iron is incorporated at lower temperatures leading to an iron rich ferrite and islands of reached Ni compounds. According to the literature data, when iron content increases, the 2θ values of the diffraction line (311) decrease. A stoichiometric nickel ferrite is formed by diffusion of Ni^{2+} into the spinel structure, process which is accomplished at approximately 500°C (a shift to higher 2θ values of 311 line).

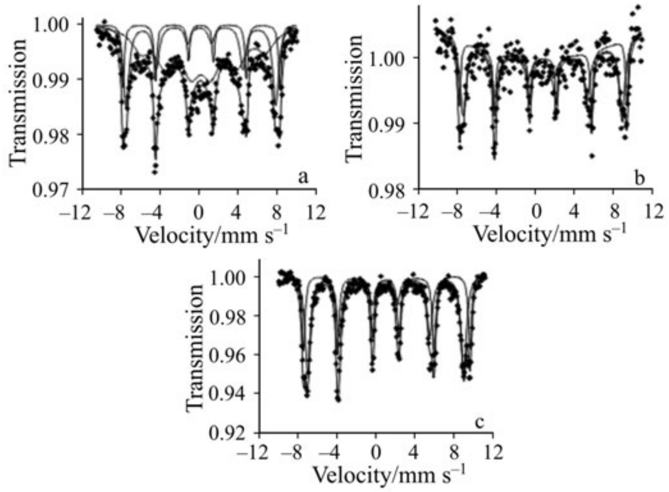

Fig. 3 Mössbauer spectra of the oxide obtained from a – $[Fe_2Ni(C_4H_4O_5)_{2.5}(OH)_2]NO_3{\cdot}5H_2O$; b – $[Fe_2Ni(C_4H_8O_3N_2)_4](NO_3)_8{\cdot}24H_2O$ and c – $(NH_4)[Fe_2Ni(C_4H_4O_5)(OH)_3]{\cdot}3H_2O$

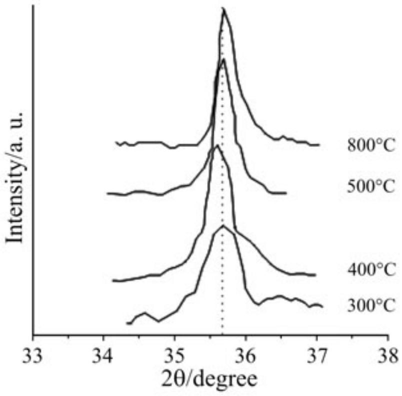

Fig. 4 X-ray diffraction reflection 311 of the spinel phase obtained at different temperatures

Thermal behaviour of $[Fe_2Ni(C_4H_8O_3N_2)_4](NO_3)_8{\cdot}24H_2O$

Five main regions of mass loss are identified in the thermal decomposition of $[Fe_2Ni(C_4H_8O_3N_2)_4](NO_3)_8{\cdot}24H_2O$ compound (Fig. 2b). A first (78–121°C) endothermic one, is assigned to a partial dehydration ($-5H_2O$, calcd/found 5.61/6.01%).

The next region (121–211°C) of mass loss (78.87%), represents the collapse of the malate lattice simultaneously with nitrate decomposition. The associated thermal effect changes from weak endo to a strong exo during reaction development, reflecting that the prevailing process shifts from an endo breakdown of the anion lattice to a vigorous oxidation of the carbonaceous and amide moieties (by Ni^{2+} and/or evolved nitrate). The TG/DTG curves reveal at least two decomposition steps. The first one (121–171°C) may be assigned to the formation of the unstable mixture iron oxohydroxyl-nickel acetate ($2FeOOH{\cdot}Ni(CH_3COO)_2$) which decompose further leading as in the first case to a carbonate intermediate.

A continuous mass loss (3.5%) ascribed to $NiCO_3 \rightarrow NiO$ change occurs in the temperature range 271–279°C. Beside Fe_2NiO_4, monometallic impurities such as Ni, $NiCO_3$, FeOOH as lepidocrit and γ-Fe_2O_3 (a well defined pattern) and a mixed iron-nickel oxohydroxid ($Fe_{0.67}Ni_{0.33}OOH$) were identified in the intermediate isolated at 300°C.

A well-defined decomposition step, assigned to water release from the oxohydroxides generated in reaction medium, likewise iron malate decomposition [10] is recorded in the 311–372°C temperature range. The Mössbauer spectrum performed at 400°C evidenced nickel ferrite as single iron containing phase (Fig. 3b).

The last decomposition step, consist in a slight mass gain (0.24%) recorded in the range 421–491°C, supporting the assumption that the sample underwent an oxidizing reaction. The appearance of nickel ferrite closely followed by a continuous mass gain, indicate the formation of a defect ferrite structure.

Thermal behaviour of $(NH_4)[Fe_2Ni(C_4H_4O_5)_3(OH)_3]{\cdot}3H_2O$

The thermal curves show two main ranges of mass loss (Fig. 2c). The first endo decomposition step (75–141°C) was assigned to a partial dehydration and ammonia evolving process ($-3H_2O$ $-NH_4OH$, calcd/found 13/01/12.01%).

The second region (141–255°C) represents the anion breakdown process with formation of the same unstable intermediate $2FeOOH\cdot Ni(CH_3COO)_2$ (calcd/found 74.26/73.5%). This compound decompose via a malonate intermediate (Table 1) in Fe_2NiO_4 (255–338°C). It is worth mentioning that at 300°C the single foreign phase detected in the oxide is the mixed oxohydroxyl $Fe_{0.67}Ni_{0.33}OOH$. The Mössbauer spectra of the oxide obtained by calcination at 400°C (Fig. 3c) exhibit only two magnetic hyperfine sextets characteristics for nickel ferrite structure. The result is confirmed by X-ray diffraction.

Discussions

On the basis of thermogravimetric and complementary measurements (IR, X-ray diffraction and Mössbauer) the following decomposition pathways may be assumed for the three studied compounds:

$$\begin{aligned}
&[Fe_2Nima_{2.5}(OH)_2]NO_3\cdot 5H_2O\\
&\xrightarrow{75\text{–}150^\circ C}[Fe_2Nima_{2.5}(OH)_2]NO_3\xrightarrow{150\text{–}240^\circ C}[Fe_2Nimal_{2.5}(OH)_3]\\
&\xrightarrow{240\text{–}320^\circ C}\begin{array}{c}\text{Mixture } Fe_2NiO_4,\\ FeOOH(\text{lepidocrit}),\ \gamma-Fe_2O_3\,(?),Ni,NiCO_3\end{array}\\
&\xrightarrow{335\text{–}595^\circ C}Fe_2NiO_4
\end{aligned}\tag{1}$$

$$\begin{aligned}
&[Fe_2Ni(C_4H_8O_3N_2)_4](NO_3)_8\cdot 24H_2O\\
&\xrightarrow{78\text{–}121^\circ C}[Fe_2Ni(C_4H_8O_3N_2)_4](NO_3)_8\cdot 19H_2O\\
&\xrightarrow{121\text{–}171^\circ C}2FeOOH\cdot Ni(CH_3COO)_2\\
&\xrightarrow{171\text{–}300^\circ C}\begin{array}{c}\text{Mixture } Fe_2NiO_4,\ (Fe_{0.67}Ni_{0.33})OOH,\\ \gamma-Fe_2O_3,Ni,NiCO_3\end{array}\\
&\xrightarrow{300\text{–}491^\circ C}Fe_2NiO_4
\end{aligned}\tag{2}$$

$$\begin{aligned}
&(NH_4)[Fe_2Nima_3(OH)_3]\cdot 3H_2O\\
&\xrightarrow{75\text{–}141^\circ C}[Fe_2Nima_3(OH)_2]\\
&\xrightarrow{141\text{–}255^\circ C}2FeOOH\cdot Ni(CH_3COO)_2\\
&\xrightarrow{255\text{–}280^\circ C}\text{Mixture } Fe_2NiO_4,(Fe_{0.67}Ni_{0.33})OOH\\
&\xrightarrow{280\text{–}380^\circ C}Fe_2NiO_4
\end{aligned}\tag{3}$$

The temperatures above the arrows are detected at a heating rate of 5°C min^{-1}, and ma and mal represent the dianions of malic respective malonic acids.

The following outcomes concerning the solid state mechanism may be pointed out:

a) The conversion process of $[Fe_2Ni(C_4H_4O_5)_{2.5}(OH)_2]NO_3\cdot 5H_2O$ compound is mildly segregative and gives a somewhat inhomogeneous distribution of Ni and Fe ions. This behavior is induced partly by the non-equivalency of the metals environments and, on the other hand by the presence NO_3^- ions. On heating, in the temperature range 300–500°C, they are incorporated into the seed spinel lattice. A good pure $NiFe_2O_4$ is obtained at 500°C/4 h.

b) Comparative with compound (**I**), the metal ions in compounds (**II**) and (**III**) are initially held in a higher state of uniform distribution. It is expected that during the rapid thermal decomposition this distribution will be largely retained. The result is a homogenous blend of $NiFe_2O_4$ and $Fe_{0.67}Ni_{0.33}OOH$, compound in which the metal ratio is the same as in ferrite. The presence of NO_3^- in compound (**II**) determines a more energetic decomposition comparative with the one underwent by compound (**III**), leading to an overheating of the sample. As a consequence, the monometallic compounds are formed in competition with $Fe_{0.67}Ni_{0.33}OOH$, and ferrite crystallization. The appearance in the decomposition progress of nickel ferrite, closely followed by a continuous mass gain, indicate the formation of a defect ferrite structure. Since the X-ray diffraction results points explicitly a spinelic structure with deviation from stoichiometry, without other spinelic foreign phases (>400°C), and taking into account the absence of Fe^{2+}, we are ready assume that a compound with the general formula $Ni_{x-\alpha}Fe_{1-x+\alpha}[Ni_{1-x}Fe_{1+x-\alpha/3*\alpha/3}]O_4$ may be formed.

c) The initial homogeneous distribution of the metallic ions is preserved during the thermal decomposition of the compound $(NH_4)[Fe_2Ni(C_4H_4O_5)_3(OH)_3]\cdot 3H_2O$, leading to a mixture of Fe_2NiO_4 and $Fe_{0.67}Ni_{0.33}OOH$. The compound's homogeneity together with its composition favors the formation of nickel ferrite, being no concentrating regions.

* * *

The research was financial supported by MATNANTECH program.

References

1 M. Brezeanu, L. Patron and M. Andruh, Polynuclear Coordination Compounds and Their Application (in Roumanian) Ed. Academiei, 1986.
2 O. Carp and E. Segal, Rev. Roum. Chim., 39 (1994) 1123.
3 O. Carp and L. Patron, Roum. Chem. Quart. Rev., (submitted).
4 O. Carp, Roum. Chem. Quart. Rev., (under press).
5 I. Mindru, L. Patron and M. Brezeanu, Roum. Chem. Quart. Rev., 4 (1996) 167.
6 O. Carp, L. Patron, A. Ianculescu, D. Crisan, N. Dragan and R. Olar, J. Therm. Anal. Cal., 72 (2003) 253.
7 O. Carp, L. Patron, G. Marinescu, G. Pascu, P. Budrugeac and M. Brezeanu, J. Therm. Anal. Cal., 72 (2003) 263.
8 N. S. Gajbhiye and S. Pasad, Thermochim. Acta, 285 (1996) 325.
9 T. V. Albu, I. Mindru, L. Patron, E. Segal and M. Brezeanu, Thermochim. Acta, 340 (1999) 235.
10 T. V. Albu, L. Patron and E. Segal, J. Therm. Anal. Cal., 48 (1997) 359.
11 P. Spacu, L. Patron, A. Butucelea, Rev. Roum. Chim., 36 (1991) 519.
12 L. Patron, O. Carp, I. Mindru and G. Marinescu, J. Therm. Anal. Cal. (submitted).

13 I. Mindru, L. Patron, O. Carp, G. Marinescu, L. Diamandescu and A. Banuta, Mat. Res. Bull. (submitted).

14 L. Patron, O. Carp, I. Mindru, G. Marinescu and E. Segal, J. Therm. Anal. Cal., 72 (2003) 281.

15 K. Nakamoto, Infrared and Raman Spectra of Inorganic and Coordination Compounds, Ed. 4, J. Wiley & Sons, 1986, p. 223.

16 A. P. B. Lever, Inorganic Electronic Spectroscopy, Elesevier Publ. Comp., Amsterdam, London, New York 1994.

17 L. Patron, O. Carp, I. Mindru and G. Grasa, J. Therm. Anal. Cal., 55 (1999) 597.

18 M. A. Mohamed, A. K. Galwey and S. Halawy, Thermochim. Acta, 323 (1998) 27.

19 C. Barriga, V. Barron, R. Gancelo, M. Garcia, J. Morales, J. L. Tirado and J. Torrent, J. Solid State Chem., 77 (1988) 132.

20 M. De Marco, X. W. Wang, R. L. Snyder, J. Simmins, S. Bayya, M. White and M. J. Naughton, J. Appl. Phys., 73 (1993) 6287.